ORGANOMETALLICS

Article

pubs.acs.org/Organometallics

Selectivity Switch in the Synthesis of Vinylgold(I) Intermediates

A. Stephen K. Hashmi,*[,†] Andreas M. Schuster,[†] Sylvain Gaillard,[‡,§] Luigi Cavallo,[∥,#] Albert Poater,[⊥] and Steven P. Nolan*[,‡]

[†]Organisch-Chemisches Institut, Ruprecht-Karls-Universität Heidelberg, Im Neuenheimer Feld 270, 69120 Heidelberg, Germany

[‡]EaStCHEM School of Chemistry, University of St Andrews, St Andrews KY16 9ST, U.K.

[§]Laboratoire de Chimie Moléculaire et Thioorganique, UMR 6507, INC3M, FR 3038, ENSICAEN-Université de Caen, 6 bd. Maréchal Juin 14050 Caen, France

[∥]Dipartimento di Chimica, Università di Salerno, Via ponte don Melillo, 84084, Fisciano, Italy

[#]KAUST Catalysis Center and Division of Chemicals and Life Sciences & Engineering 4700, King Abdullah University of Science and Technology, Thuwal 23955-6900, Kingdom of Saudi Arabia

[⊥]Catalan Institute for Water Research (ICRA), H2O Building, Scientific and Technological Park of the University of Girona, Emili Grahit 101, E-17003 Girona, Spain

Supporting Information

ABSTRACT: An unexpected regioselectivity reversal was observed in the synthesis of vinylgold(I) complexes from propargyl carboxamides. The use of [Au(IPr)(OH)] affords preferentially vinylgold(I) complexes resulting from a 5-exo-dig cyclization, whereas the use [Au(IPr)]$^+$ species, generated in situ starting from [Au(IPr)(Cl)] and AgOTf, leads to vinylgold(I) complexes which form via a 6-endo-dig cyclization, This unexpected "selectivity switch" for this cyclization led us to propose two different reaction pathways enabling the formation of the two different products. One mechanism involves the [Au(IPr)]$^+$ species with "classical" π activation of the alkyne framework of the carboxamides, and the second represents an "unusual" use of the basic Brønsted character of [Au(IPr)(OH)]. Mechanistic and DFT studies support the mechanistic hypotheses.

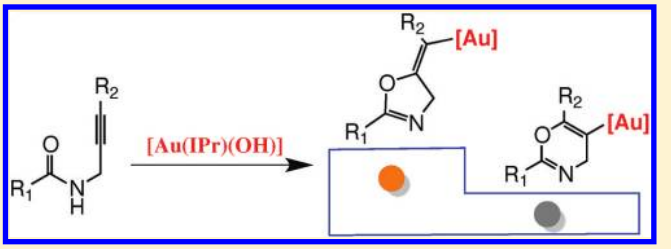

INTRODUCTION

Gold-catalyzed organic transformations represent a truly prolific area of research in organic chemistry.[1] This is certainly due to the wide range of organic transformations gold has successfully mediated thus far. Of utmost importance in such reactions is the propensity of gold to act as an electrophilic activator for C−C multiple bonds.[2] It is commonly accepted that nucleophiles can attack C−C multiple bonds that have been activated by cationic gold(I) complexes. For an in-depth understanding of the mechanism involving these cationic gold(I) complexes, trapping such intermediates has become a desirable goal that some may characterize as essential.[3] With this aim in mind, Hashmi et al. succeeded in the isolation of a vinylgold(I) complex intermediate (**2a**)[4] resulting from a 6-endo-dig cyclization of *N*-propargyl carboxamides (**1a**)[5] (eq 1).

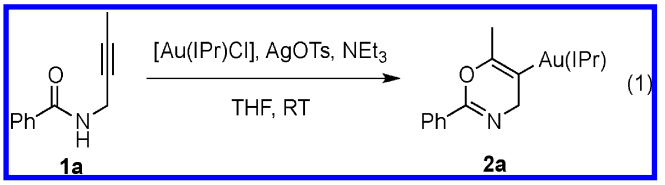

In a related area, Nolan and co-workers have reported the synthesis of novel [Au(NHC)(OH)] complexes (NHC = N-heterocyclic carbene),[6] one of which has been demonstrated to act as a versatile synthon in organometallic chemistry[7] as well as proving quite useful in homogeneous catalysis.[8] In the course of these synthetic and catalytic studies, [Au(IPr)(OH)] (**3**) (IPr = 1,3-bis(2,6-diisopropylphenyl)imidazol-2-ylidene) displayed interesting Brønsted basic properties which were envisaged to possibly trigger novel reactivity.[6,8e,f] The use of [Au(IPr)(OH)] (**3**) as a mechanistic probe in the cyclization of propargyl carboxamides **1** is now examined and compared to the previously reported procedure leading to vinylgold(I) intermediates.[4d] Herein, results on new selectivity brought about by the use of **3** for cyclization of *N*-propargyl carboxamide derivatives **1** are presented.

RESULTS AND DISCUSSION

Various *N*-propargyl carboxamides **1**, bearing an internal alkyne, were prepared and reacted with **3** (condition A) or with in situ generated cationic [Au(IPr)]$^+$ (from [AuCl(IPr)] and AgOTs in presence of triethylamine) (condition B) (Table 1). Results of the selectivity between the 5-exo-dig and the 6-

Received: October 10, 2011
Published: October 28, 2011

   dx.doi.org/10.1021/om2009556|*Organometallics* 2011, 30, 6328−6337

Table 1. Synthesis of Vinylgold(I) Complexes 2 and 4 from *N*-Propargyl Carboxamides 1[a]

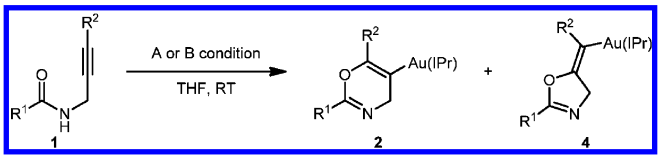

Entry	R^1	R^2	Cond.	Yield (%)	Selectivity (**2** / **4**)	Entry	R^1	R^2	Cond.	Yield (%)	Selectivity (**2** / **4**)
1	Ph	Me	A	>99	**2a** / **4a** (0.14 / 1)	11		Me	A	>99	**2f** / **4f** (0.14 / 1)
2	Ph	Me	B	82	**2a** / **4a** (1 / 0.04)	12		Me	B	76	**2f** / **4f** (1 / 0.17)
3	Ph	Et	A	>99	**2b** / **4b** (0.16 / 1)	13		Me	A	>99	**2g** / **4g** (0.15 / 1)
4	Ph	Et	B	81	**2b** / **4b** (1 / 0.2)	14		Me	B	58	**2g** / **4g** (1 / 0.5)
5	Ph	*n*Pr	A	>99	**2c** / **4c** (0.14 / 1)	15	Ph	Ph	A	>99	**2h** / **4h** (0 / 1)
6	Ph	*n*Pr	B	85	**2c** / **4c** (1 / 0.26)	16	Ph	Ph	B	60	**2h** / **4h** (0 / 1)
7	Ph	*n*Bu	A	>99	**2d** / **4d** (0.14 / 1)	17	Ph		A	>99	**2i** / **4i** (0 / 1)
8	Ph	*n*Bu	B	88	**2d** / **4d** (1 / 0.31)	18	Ph		A	Dec.	-
9		Me	A	>99	**2e** / **4e** (0.22 / 1)	19	Ph		A	>99	**2k** / **4k** (0 / 1)
10		Me	B	81	**2e** / **4e** (1 / 0.07)						

[a]Conditions: (A) reaction carried out in a NMR tube with propargyl carboxamide **1** (85 μmol) and [Au(IPr)(OH)] (**3**; 85 μmol) in THF-d_8 at room temperature; (B) reaction carried out in a Schlenk tube with [Au(IPr)Cl] (161 μmol), AgOTs (161 μmol), triethylamine (100 μL), and propargyl carboxamide **1** (153 μmol) in dry THF at room temperature.

endo-dig cyclization of compounds **1**, respectively yielding the vinylgold(I) complexes **4** and/or **2**, are presented in Table 1.

All propargyl carboxamides **1a**−**h** were fully converted into a mixture of vinylgold(I) complexes **2** and **4** under both reaction conditions (Table 1, entries 1−16). Propargyl carboxamides **1i**−**k** were only subjected to reaction conditions A, and only compound **1j** did not furnish the expected vinylgold(I) complexes **2j** and/or **4j**, instead yielding decomposition of the starting material (Table 1, entry 18). Nevertheless, **1i**,**k** gave only the vinylgold(I) complexes **4i**,**k**, respectively. Noteworthy, all propargyl carboxamide derivatives **1** gave quantitatively a mixture of **2** and **4** under reaction conditions A, whereas reaction conditions B afforded these mixtures in yields ranging from 58% to 88% (Table 1, entries 1−16). The most important observation was the reversal in expected regioselectivity between reaction conditions A and B. Indeed, using conditions A, the major vinylgold(I) complexes **4** result from a 5-exo-dig cyclization, whereas under conditions B, the major products formed were vinylgold(I) complexes **2**, which are formed via a 6-endo-dig cyclization. Among these observations, only one exception in this reactivity trend was observed, for **1h**, which selectively afforded, using either protocol, the vinylgold(I) complex **4h** (Table 1, entries 15 and 16). Finally, **3** (conditions A) proved more selective than $[Au(IPr)]^+$ (conditions B), as better **4**/**2** ratios were obtained using this well-defined complex. The electronic effects of substituents R^1 and R^2 were both obviously involved in this selectivity. Indeed, when R^1 remained constant, if R^2 was an alkyl group, formation of **2** was favored (Table 1, entries 2, 4, 6, and 8), whereas the presence of an aryl group favored the formation of **4** (Table 1, entry 16). Such dramatic selectivity does not appear so clear-cut under reaction conditions A. Nevertheless, when R^1 and R^2 are two aromatic

dx.doi.org/10.1021/om2009556|*Organometallics* 2011, 30, 6328−6337

groups, total selectivity in favor of **4** was observed (Table 1, entries 15, 17, and 19). This was confirmed when **5** (bearing two alkynylcarboxamide frameworks substituted at both R^1 and R^2 positions by aromatic groups) was employed. Indeed, under conditions A, **5** afforded quantitatively and selectively the divinylgold(I) complex **6**, resulting from two 5-exo-dig cyclizations (eq 2).

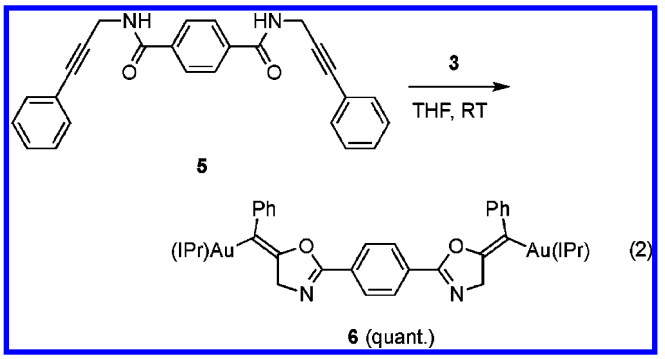

(2)

The *selectivity switch* observed with neutral **3**, possessing basic properties, in comparison to the use of a "classical" cationic gold(I) source raised questions about the mechanistic pathway preferred when **3** is employed. Under regime B, the regioselectivity observed in favor of the 6-endo-dig cyclization[4d] can be attributed to electronic effects. Indeed, the inductive effect, brought about by the terminal substituent, leads to a positive partial charge on C_a instead of C_b during the π activation of the alkyne, resulting in the selectivity observed (Scheme 1). To support this argument, when the inductive effect is absent, which is the case when a terminal alkyne is employed, this reaction leads to the sole formation of the 5-exo-dig cyclized product **4** (Scheme 1).[5]

Therefore, to understand this *switch* in regioselectivity in favor of **4** when reactions were performed under conditions A, attempts to observe intermediate(s) were carried out using ^{1}H NMR spectroscopy. Compounds **1i** and **3** were introduced into an NMR tube, and spectra were recorded every 4 min (THF-d_8, 298 K, 300.13 MHz, NS = 64, DS = 2) (Figure 1).

Initial ^{1}H NMR spectra revealed immediate formation of a new intermediate (**7i**) attributed to the deprotonated **1i** with a [Au(IPr)] group N-ligated. Then, **7i** disappeared in favor of the formation of **4i**. This observation is in good agreement with the basic properties displayed by **3**. Indeed, **3** can deprotonate compounds with pK_a(DMSO) up to 30.3 pK_a units.[8f] In view of this acid–base reactivity, the pathway leading to the cyclization appears clear. The question we next tackled was by which pathway **7** evolved into **4**.

The gold-catalyzed cyclization of 2-alkynylphenol (**8**) leading to furans has already been reported.[9] Formation of vinylgold(I) from 2-alkynylphenol (**8**) and 2-alkylaniline (**11**) is also known to proceed in the presence of cationic gold complexes.[4a] Therefore, it appeared worthwhile to examine the reactivity differences between **3** and cationic gold(I) leading to the formation of vinylgold(I) complexes **9** and **12** obtained from 2-alkynylphenol **8** and 2-alkylaniline **11**, respectively. Gratifyingly, compounds **8** and **11** in the presence of **3** afforded the corresponding vinylgold(I) complexes **9** and **12**, respectively (eqs 3 and 4).

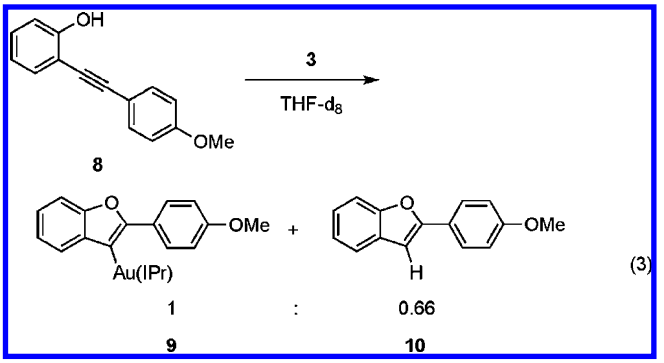

(3)

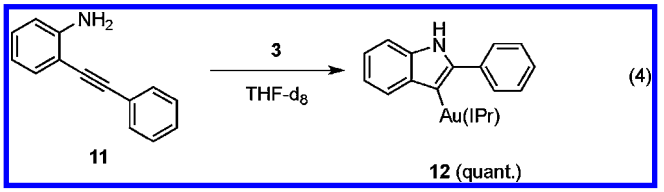

(4)

The pK_a values for phenol or aniline clearly indicate these substrates compatible with a deprotonation reaction by **3**.[10] The reactions above clearly show that the C–C triple bond is capable of being inserted into Au–O and Au–N bonds. Thereafter, the proto-deaurated compound **10**[4a] was observed, which could originate from the hydrolysis of the Au–C bond[4d] by the water generated from the deprotonation of **10** by **3**. As water cannot be involved in the proto-deauration when conditions B are used, a complementary experiment using TsOH for the cleavage of this Au–C bond in **4h** was undertaken (eq 5).

Unexpectedly, ring opening of **4h** occurs and **1h** is regenerated with concomitant formation of [Au(IPr)][OTs].

Scheme 1. Proposed Reaction Mechanism for the Formation of Complexes 2 and 4 in the Presence of a Cationic Gold(I) Source

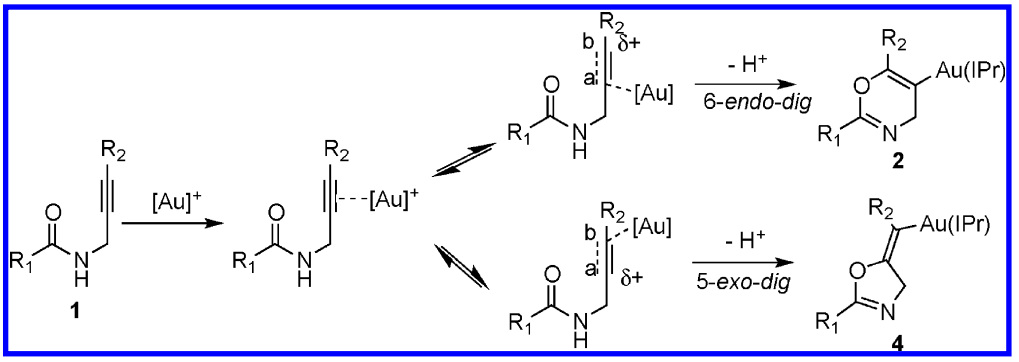

dx.doi.org/10.1021/om2009556|*Organometallics* 2011, 30, 6328–6337

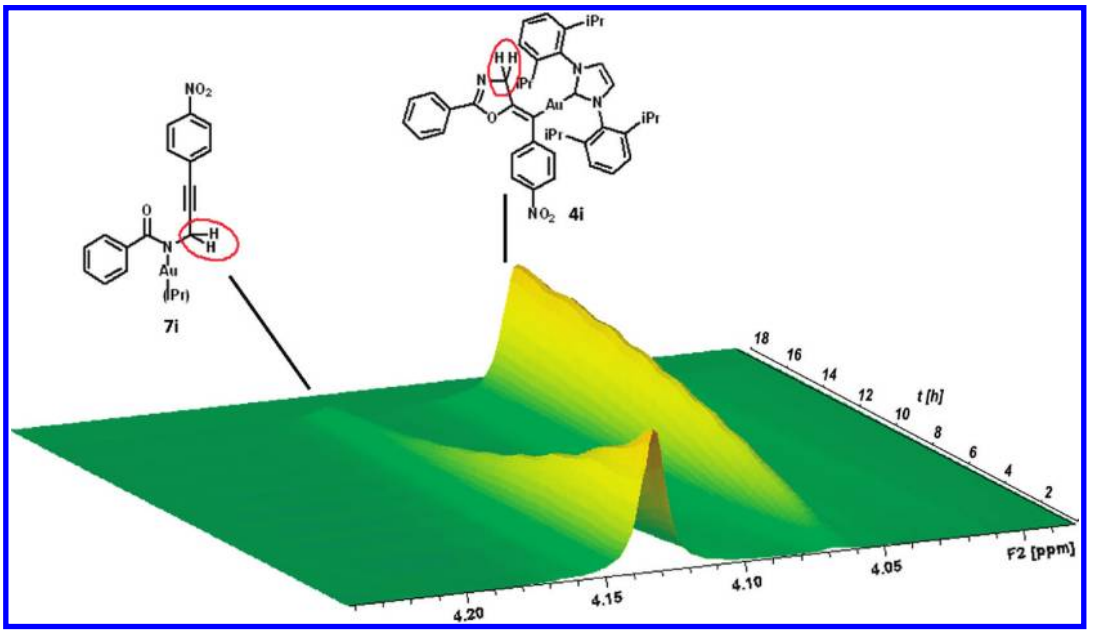

Figure 1. Isomerization of amide gold(I) complex **7i** into the vinylgold(I) complex **4i**.

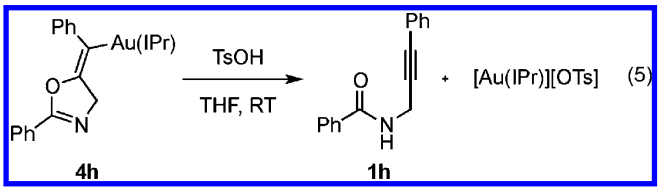

It is worth noting that no interconversion of **4h** into **2h** was observed. This is not surprising, as these reaction conditions do not lead to the reaction conditions used in Table 1 with conditions B. This experiment highlights the crucial role of triethylamine under conditions B, which traps the liberated proton during the course of the reaction and avoids the re-formation of the starting material **1h**. Finally, the absence of acidolysis of the Au−C bond in complex **4h** by TsOH is due to the basic character of the nitrogen atom of the oxazole, which reacts with the strong Brønsted acid TsOH.[4a] This led us to consider these vinylgold(I) complexes as vinyl anions highly stabilized by very sterically demanding cations. To test this hypothesis, attempts to generate this vinyl anion by reacting iodovinyloxazole (**13**) with *n*-BuLi followed by addition of water to afford the oxazole derivative **14** or [Au(IPr)Cl] to obtain **4h** was achieved (Scheme 2). After **13** was treated with *n*-BuLi and the preformed vinyl anion was quenched with water, oxazole **14** and ring-opening product **1h** were observed in a 1:1 ratio. The same reactivity was observed when water was replaced by [Au(IPr)Cl]. Indeed, under these conditions, a mixture of **4h** and the amidogold(I) complex **7h** was obtained in a 1:1 ratio. These two experiments revealed the instability of the vinyl anion when lithium is the countercation, yielding the ring-opened product. This result is in agreement with the experiment involving **4h** in the presence of TsOH, where the acid proton activates the oxazole nitrogen to afford the ring-opened product **1h**.

Finally, these experiments led us to propose a mechanism for the formation of **4**. Initially, **1** is deprotonated in the presence of [Au(IPr)(OH)] (**3**), affording as an intermediate the amidogold complex **7**, observed by ^{1}H NMR spectroscopy (Figure 1). Then, **7** is involved in an equilibrium with the amidogold complex intermediate **15**, which could be stabilized by coordination to the alkyne moiety.

Scheme 2. Evolution of the Vinyloxazole Anion in the Presence of Water or [Au(IPr)Cl]

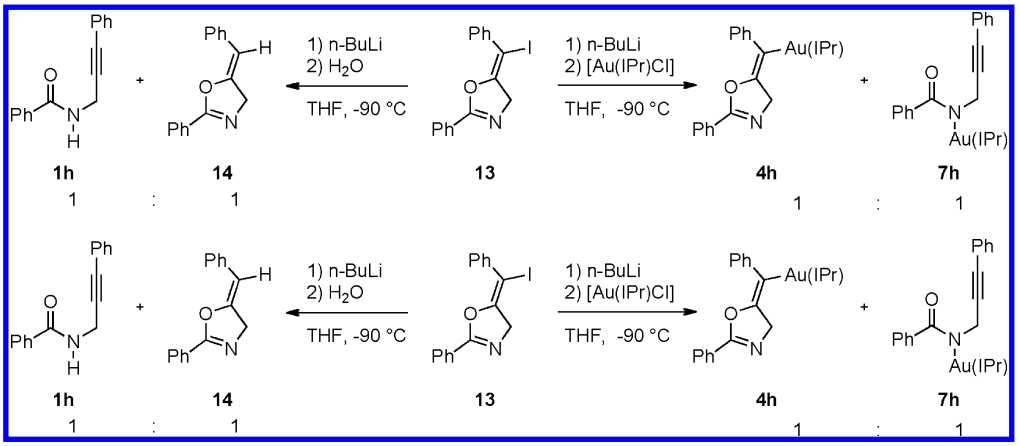

dx.doi.org/10.1021/om2009556|*Organometallics* 2011, 30, 6328−6337

DFT calculations permit us to draw a complete picture using the experimental information at hand, and energy profiles are presented in Figures 2 and 3.[11] Focusing on the reactivity of **1h**

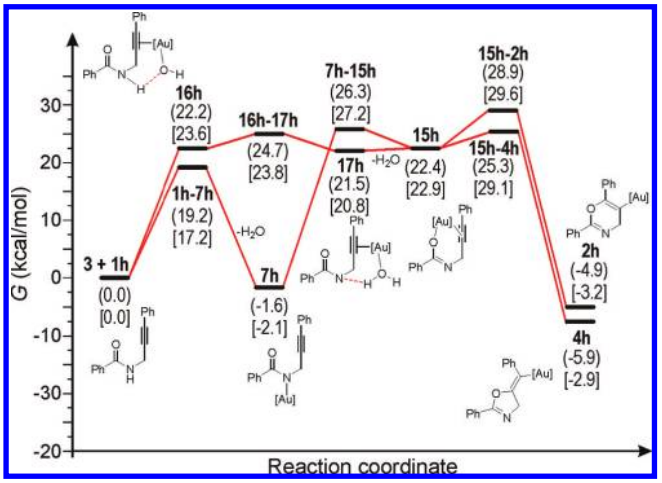

Figure 2. DFT energy profile for the cyclization of **1h** promoted by **3** (energy values in parentheses). The energy values for the cyclization of **1a** are reported in brackets. [Au] represents [Au(IPr)].

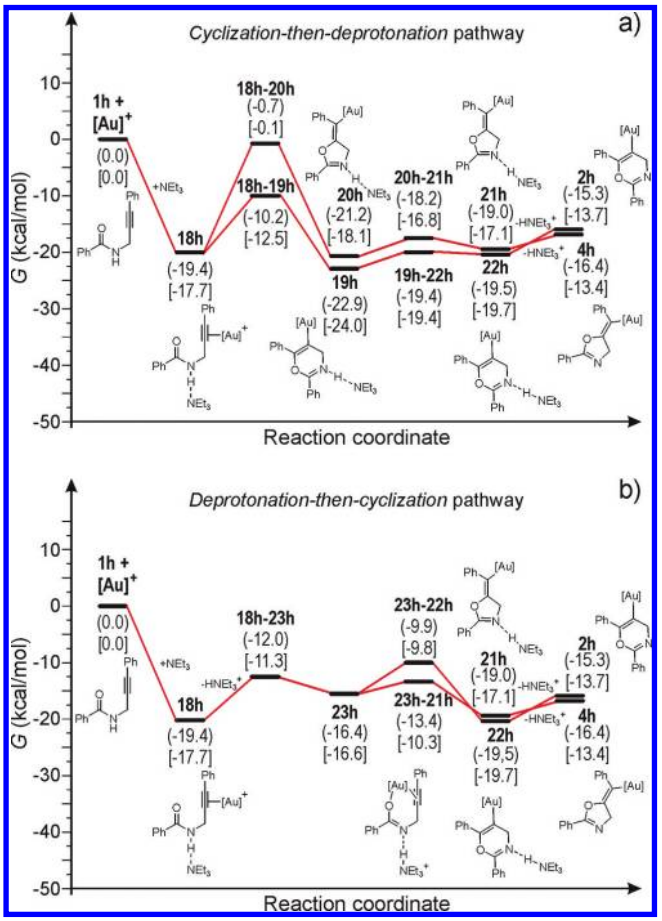

Figure 3. DFT energy profiles for the cyclization of **1h** promoted by the cationic $[Au(IPr)]^+$ species (energy values in parentheses). Energy values for the cyclization of **1a** are reported in brackets. [Au] represents [Au(IPr)].

with neutral **3**, formation of **7h** with concomitant release of a water molecule requires overcoming a barrier of 19.2 kcal/mol (see Figure 2). Structure **7h** is 1.6 kcal/mol more stable than the starting neutral species **3** plus free **1h** and is the resting state of the reaction pool. The key intermediate **15h**, at 22.4 kcal/mol in energy above **3** + **1h**, is formed through the rather high energy transition state **7h-15h**, 27.9 kcal/mol above the resting state **7h**. However, the key intermediate **15h** can be also reached via coordination of the alkyne functionality of **1h** to the gold center of **3** to yield **16h**, an endergonic step costing 22.2 kcal/mol, followed by a low-energy proton transfer step through transition state **16h-17h**, which leads to intermediate **17h**, lying 21.5 kcal/mol above **3** + **1h**. Loss of the coordinated water molecule finally leads to intermediate **15h**. Considering that transition state **7h-15h** is only 1.6 kcal/mol above transition state **16h-17h**, calculations suggest that **15h** can be formed both along the sequence **3** + **1h** →**16h** → **17h** → **15h** and along the sequence **3** + **1h** → **7h** → **15h**. Furthermore, **7h** can react reversibly with a liberated H_2O molecule to form **3** + **1h**, thus allowing the initially formed **7h** to reach the key intermediate **15h** through the slightly more stable transition state **16h-17h** rather than the slightly higher in energy transition state **7h-15h**.

The regioselectivity in favor of the 5-exo-dig pathway occurs at the level of the rate-determining cyclization step, with transition state **15h-4h**, some 3.6 kcal/mol below transition state **15h-2h**. At the product level, the five-membered Au species **4h** is only 1.0 kcal/mol more stable than the six-membered Au species **2h**. The higher stability of transition state **15h-4h** originates from the polarity of the alkyne bond, induced by the Ph group. Natural population analysis results with charges of −0.114e and −0.027e on the C1 and C2 atoms of **15h**, which drives O attack toward the less negatively (more positively) charged C2 atom. Similar results are obtained with substrate **1a** (see the numbers in brackets in Figure 2). In short, the data reported in Figure 2 provide a rationale for the experimentally observed preferential 5-cyclization promoted by neutral **3**.

Moving to cyclization in the presence of the cationic $[Au(IPr)]^+$ species, the corresponding energy profiles are shown in Figure 3. After initial coordination of **1h** to the cationic Au species, leading to intermediate **18h**, with a release of 19.4 kcal/mol, the question is whether cyclization occurs before or after deprotonation of the NH functionality of **1h** by NEt_3, leading thus to a competition between *cyclization-then-deprotonation* and *deprotonation-then-cyclization* pathways. Along the cyclization-then-deprotonation pathway (Figure 3a), the 6-endo-dig cyclization transition state **18h-19h** is strongly favored over the 5-exo-dig cyclization transition state **18h-20h**, which is calculated to be 9.5 kcal/mol higher in energy. Deprotonation of the NH functionality of the cyclized intermediates **19h** and **20h** with the transfer of the proton from the substrate to the H-bonded NEt_3 is not an issue, with an energetic cost of less than 5 kcal/mol, and leads to the intermediates **21h** and **22h**. Dissociation of $HNEt_3^+$, perhaps assisted by the tosylate, liberates the final products **2h** and **4h**. Along the deprotonation-then-cyclization pathway (Figure 3b), NEt_3 deprotonates the NH functionality of the coordinated substrate in **18h** prior cyclization. This step proceeds through transition state **18h-23h**, requiring 7.4 kcal/mol, and leads to the neutral Au species **23h** with a $HNEt_3^+$ molecule H-bonded to the N atom of the substrate. Cyclization from **23h** gives the intermediates **21h** and **22h** through transition states **23h-21h** and **23h-22h**. As in Figure 3a, dissociation of the H-bonded $HNEt_3^+$ from **21h** and **22h** liberates the final products **4h** and **2h**. Consistent with the

dx.doi.org/10.1021/om2009556|*Organometallics* 2011, 30, 6328–6337

energetic plot of Figure 2, a neutral Au species such as **23h** interacting with a $HNEt_3^+$ molecule H-bonded to the N atom of the substrate, 5-exo-dig cyclization is favored over 6-endo,dig cyclization. This preference is calculated to be 3.5 kcal/mol, which is nearly identical with the preference of 3.6 kcal/mol in favor of the 5-exo-dig cyclization in the case of **1h** cyclization promoted by neutral **3** (see Figure 2), indicating a minor effect of the H-bonded $HNEt_3^+$ molecule. Focusing on a comparison between the cyclization-then-deprotonation and deprotonation-then-cyclization pathways, it is noteworthy that, with the exception of transition state **18h-20h** leading to **4h** along the cyclization-then-deprotonation pathway, the key transition states **18h-23h**, **23h-21h**, **23h-22h**, and **18h-19h** are of similar energy and are thus in competition. This indicates that in the case of a cationic Au species the 5-exo-dig product **4h** can be formed along both the cyclization-then-deprotonation and deprotonation-then-cyclization pathways, whereas the 6-endo-dig product **2h** can be formed along the cyclization-then-deprotonation pathway only. However, as an initial step the deprotonation is favored by 1.8 kcal/mol with respect to the competitive cyclization. A similar chemical scenario is calculated when **1a** is the substrate; see the energy values in brackets in Figure 3. In summary, calculations provide a rationale for the increased amount of six-membered vinylgold products promoted by the cationic $[Au(IPr)]^+$ species. Finally, in the case of the deprotonation-then-cyclization pathway, formation of the five-membered vinylgold species is favored over formation of the six-membered vinylgold species by 3.5 kcal/mol in the case of **1h**, whereas this preference is reduced to only 0.5 kcal/mol in the case of **1a**. This result is also consistent with the experimental finding that **1h** cyclization promoted by the cationic $[Au(IPr)]^+$ species yields only the five-membered vinylgold species **4h**.

To further support the computational work and proposed reaction pathways, the kinetics of formation of **4i** from **1i** were investigated under conditions A at four temperatures (50, 40, 25, and 10 °C) and an Arrhenius plot constructed (see the Supporting Information). The effective energy E_A was calculated as 24.2 kcal/mol, which is in good agreement with the value estimated by DFT calculations of compound **1h** converting into vinylgold(I) **4h** passing through intermediate **15h**. This compares to the theoretical value for the activation energy of 22.4 kcal/mol and is consistent with the experimental value if substituent variations between **1h** and **1i** are considered.

■ CONCLUSION

An unprecedented *regioselectivity switch* in vinylgold(I) complex synthesis from propargyl carboxamides **1** as a function of the gold(I) source has been reported. Indeed, the use of **3** preferentially leads, via a 5-exo-dig cyclization, to vinylgold(I) complexes **4**, whereas the use of the $[Au(IPr)]^+$ species provided, via a 6-endo-dig cyclization, leads to complexes of type **2**. This switch in regioselectivity can be attributed to the basic properties of [Au(IPr)(OH)] (**3**), confirming our hope that this stable and easily synthesized complex might lead to novel reactivities. Further investigations focusing on the use of **3** and related complexes are ongoing in our laboratories.

■ EXPERIMENTAL SECTION

General Considerations. All reactions were carried out in air unless otherwise stated. In such exceptions, manipulations were performed using standard Schlenk techniques using an inert atmosphere of dry argon or in a MBraun glovebox containing dry argon and less than 1 ppm of oxygen. Anhydrous solvents were either distilled from appropriate drying agents or purchased from Aldrich and degassed prior to use by purging with dry argon and kept over molecular sieves. Solvents for NMR spectroscopy were degassed with argon and dried over molecular sieves. NMR spectra were recorded on a 400 MHz Varian Gemini spectrometer. Elemental analyses were performed by St Andrews analytical services. Complex **3** was prepared according to the procedure described in the literature.[6] Chemicals were purchased from the indicated supplier in the indicated purity: triethylamine (Acros, 99%), [AuCl(IPr)] (Strem, 95%). Dry solvents were obtained from a Braun MB-SPS 800 solvent purification system. Deuterated solvents were purchased from Euriso-top and used from the bottle without further drying. NMR spectra were recorded on a Bruker Avance DRX-300 MHz spectrometer. Mass spectra were taken with a JEOL JMS-700 spectrometer. As a FAB matrix either NBA (3-nitrobenzyl alcohol) or NPOE (*o*-nitrophenyl octyl ether) was used. IR spectroscopy was processed on a FT-IR Bruker Vector 22. IUPAC names of the compounds were determined with ACDLabs 12.0.

General Procedure for the Synthesis of Vinylgold Compounds (GP1). In a NMR tube propargylamide and [Au(OH)(IPr)] (**3**) were dissolved in THF-d_8 at room temperature. The reaction was monitored by NMR. To obtain the product, the solvent was removed at the rotary evaporator without heating.

General Procedure for the Synthesis of Vinylgold Compounds (GP2). In a 25 mL Schlenk tube 100 mg (161 μmol) of [AuCl(IPr)] and 45 mg (161 μmol) of AgOTs were dissolved in 6 mL of dry THF and stirred for 1 h. Then 100 μL of triethylamine and 153 mmol amide were added. The reaction mixture was stirred for a further 16 h at room temperature, filtered over a small column of basic Alox, and washed with 50 mL of dry THF. To obtain the product, the solvent was removed at the rotary evaporator without heating.

Synthesis of 4a and 2a. According to GP1, 14.7 mg (85.0 μmol) of *N*-(but-2-ynyl)benzamide and 51.2 mg (85.0 μmol) of [Au(OH)(IPr)] (**3**) were used. After 1 day, **4a** and **2a** were obtained as a white foam in quantitative yield (**4a**/**2a** = 1/0.14). According to GP2, 26.3 mg (152 μmol) *N*-(but-2-ynyl)benzamide was used. After 1 d, **4a** and **2a** were obtained as a white foam in 82% yield (Ratio **4a**/**2a** = 0.04/1).

*{1,3-Bis[2,6-bis(propan-2-yl)phenyl]-1,3-dihydro-2H-imidazol-2-ylidene}[(1E)-1-(2-phenyl-1,3-oxazol-5(4H)-ylidene)ethyl]gold (**4a**).* ^{1}H NMR (300 MHz, THF-d_8): δ 1.23 (d, *J* = 7.0 Hz, 12 H), 1.40 (d, *J* = 7.0 Hz, 12 H), 1.57 (t, *J* = 2.5 Hz, 3 H), 2.61−2.77 (m, 4 H), 3.88 (q, *J* = 2.5 Hz, 2 H), 7.25−7.40 (m, 7 H), 7.44−7.57 (m, 4 H), 7.79−7.88 (m, 2 H). ^{13}C NMR (75 MHz, THF-d_8): δ 21.05 (q), 24.30 (q, 4 C), 25.06 (q, 4 C), 29.84 (d, 4 C), 59.08 (t), 124.38 (d, 2 C), 124.77 (d, 4 C), 128.45 (d, 2 C), 128.86 (d, 2 C), 129.19 (s), 130.72 (s), 131.06 (d, 2 C), 131.24 (d), 136.18 (s, 2 C), 146.96 (s, 4 C), 151.11 (s), 163.96 (s), 198.08 (s).

*{1,3-bis[2,6-bis(propan-2-yl)phenyl]-1,3-dihydro-2H-imidazol-2-ylidene}(6-methyl-2-phenyl-4H-1,3-oxazin-5-yl)gold (**2a**).* ^{1}H NMR (300 MHz, THF-d_8): δ 1.23 (d, *J* = 7.0 Hz, 12 H), 1.38 (d, *J* = 7.0 Hz, 12 H), 1.43 (t, *J* = 1.6 Hz, 3 H), 2.61−2.77 (m, 4 H), 3.68 (q, *J* = 1.6 Hz, 2 H), 7.14−7.25 (m, 4 H), 7.25−7.40 (m, 3 H), 7.44−7.57 (m, 4 H), 7.79−7.88 (m, 2 H). ^{13}C NMR (75 MHz, THF-d_8): δ 22.06 (q), 24.30 (q, 4 C), 25.03 (q, 4 C), 30.82 (d, 4 C), 53.04 (t), 124.45 (d, 2 C), 124.77 (d, 4 C), 127.58 (d, 2 C), 128.30 (d, 2 C), 130.13 (d), 131.02 (d, 2 C), 135.92 (s), 136.14 (s, 2 C), 145.92 (s), 146.92 (s, 4 C), 147.25 (s), 153.96 (s), 197.90 (s). HRMS (FAB(+), matrix NPOE): $[C_{38}H_{47}ON_3Au]^+$ calcd 758.3385, found 758.3358. IR (KBr): $\tilde{\nu}$ (cm^{-1}) 2962, 2927, 2868, 2282, 1680, 1470, 1459, 1415, 1385, 1365, 1337, 1285, 1147, 1102, 1067, 1024, 804, 758, 696, 512, 501.

Synthesis of 4b and 2b. According to GP1, 14.6 mg (85.0 μmol) of *N*-(pent-2-ynyl)benzamide and 51.2 mg (85.0 μmol) of [Au(OH)(IPr)] (**3**) were used. After 1 day, **4b** and **2b** were obtained as a pale yellow foam in quantitative yield (**4b**/**2b** = 1/0.16). According to GP2, 28.6 mg (152 μmol) of *N*-(pent-2-ynyl)benzamide was used. After 1 day, **4b** and **2b** were obtained as a pale yellow foam in 81% yield (**4b**/**2b** = 0.20/1).

*{1,3-Bis[2,6-bis(propan-2-yl)phenyl]-1,3-dihydro-2H-imidazol-2-ylidene}[(1E)-1-(2-phenyl-1,3-oxazol-5(4H)-ylidene)propyl]gold (**4b**).* ^{1}H NMR (300 MHz, THF-d_8): δ 0.56 (t, *J* = 7.6 Hz, 3 H), 1.23

(d, J = 6.9 Hz, 12 H), 1.39 (d, J = 6.9 Hz, 12 H), 2.11 (tq, J = 7.6 Hz, J = 2.1 Hz, 2 H), 2.60−2.78 (m, 4 H), 3.86 (t, J = 2.1 Hz, 2 H), 7.26−7.38 (m, 7 H), 7.45−7.56 (m, 4 H), 7.76−7.84 (m, 2 H). ^{13}C NMR (75 MHz, THF-d_8): δ 17.47 (q), 24.38 (q, 4 C), 25.01 (q, 4 C), 28.25 (t), 29.86 (d, 4 C), 58.93 (t), 124.31 (d, 2 C), 124.75 (d, 4 C), 128.44 (d, 2 C), 128.85 (d, 2 C), 131.03 (d, 2 C), 131.23 (d), 136.24 (s, 2 C), 137.97 (s), 146.72 (s), 147.01 (s, 4 C), 150.01 (s), 163.97 (s), 198.91 (s).

{1,3-Bis[2,6-bis(propan-2-yl)phenyl]-1,3-dihydro-2H-imidazol-2-ylidene}(6-ethyl-2-phenyl-4H-1,3-oxazin-5-yl)gold ***(2b)***. ^{1}H NMR (300 MHz, THF-d_8): δ 0.75 (t, J = 7.5 Hz, 3 H), 1.23 (d, J = 6.9 Hz, 12 H), 1.38 (d, J = 6.9 Hz, 12 H), 1.75 (tq, J = 7.6 Hz, J = 0.7 Hz, 2 H), 2.60−2.78 (m, 4 H), 3.68 (t, J = 0.7 Hz, 2 H), 7.26−7.38 (m, 7 H), 7.45−7.56 (m, 4 H), 7.76−7.84 (m, 2 H). ^{13}C NMR (75 MHz, THF-d_8): δ 13.93 (q), 24.33 (q, 4 C), 25.03 (q, 4 C), 29.86 (d, 4 C), 30.61 (t), 53.06 (t), 124.43 (d, 2 C), 124.77 (d, 4 C), 127.57 (d, 2 C), 128.32 (d, 2 C), 130.71 (s), 131.01 (d, 2 C), 131.18 (d), 136.15 (s, 2 C), 146.63 (s), 146.93 (s, 4 C), 151.70 (s), 154.12 (s), 197.97 (s). HRMS (FAB(+), matrix NPOE): $[C_{39}H_{49}ON_3Au]^+$ calcd 772.3541, found 772.3543. IR (KBr): $\tilde{\nu}$ (cm^{-1}) 3440, 2962, 2926, 2868, 1675, 1653, 1632, 1471, 1459, 1414, 1384, 1364, 1336, 1086, 1062, 1043, 1025, 804, 758, 694.

Synthesis of 4c and 2c. According to GP1, 17.1 mg (85.0 μmol) of *N*-(hex-2-ynyl)benzamide and 51.2 mg (85.0 μmol) of [Au(OH)(IPr)] (**3**) was used. After 1 day, **4c** and **2c** were obtained as a white foam in quantitative yield (**4c**/**2c** = 1/0.14). According to GP2, 30.8 mg (152 μmol) of *N*-(hex-2-ynyl)benzamide was used. After 1 day, **4c** and **2c** were obtained as a white foam in 85% yield (**4c**/**2c** = 0.26/1).

{1,3-Bis[2,6-bis(propan-2-yl)phenyl]-1,3-dihydro-2H-imidazol-2-ylidene}[(1E)-1-(2-phenyl-1,3-oxazol-5(4H)-ylidene)butyl]gold ***(4c)***. ^{1}H NMR (300 MHz, THF-d_8): δ 0.58 (t, J = 7.4 Hz, 3 H), 0.91−1.05 (m, 2 H), 1.23 (d, J = 6.9 Hz, 12 H), 1.39 (d, J = 6.9 Hz, 12 H), 2.10 (tt, J = 7.1 Hz, J = 2.1 Hz, 2 H), 2.61−2.78 (m, 4 H), 3.86 (t, J = 2.1 Hz, 2 H), 7.17−7.38 (m, 7 H), 7.45−7.56 (m, 4 H), 7.75−7.86 (m, 2 H). ^{13}C NMR (75 MHz, THF-d_8): δ 14.73 (q), 24.40 (q, 4 C), 24.96 (q, 4 C), 26.05 (t), 29.85 (d, 4 C), 37.40 (t), 59.01 (t), 124.28 (d, 2 C), 124.75 (d, 4 C), 128.44 (d, 2 C), 128.84 (d, 2 C), 130.75 (s), 131.02 (d, 2 C), 131.21 (d), 135.95 (s), 136.26 (s, 2 C), 147.01 (s, 4 C), 150.66 (s), 164.01 (s), 198.89 (s).

{1,3-Bis[2,6-bis(propan-2-yl)phenyl]-1,3-dihydro-2H-imidazol-2-ylidene}(6-butyl-2-phenyl-4H-1,3-oxazin-5-yl)gold ***(2c)***. ^{1}H NMR (300 MHz, THF-d_8): δ 0.64 (t, J = 7.4 Hz, 3 H), 0.91−1.05 (m, 2 H), 1.23 (d, J = 6.9 Hz, 12 H), 1.39 (d, J = 6.9 Hz, 12 H), 1.79 (tt, J = 7.1 Hz, J = 0.8 Hz, 2 H), 2.61−2.78 (m, 4 H), 3.67 (t, J = 0.8 Hz, 2 H), 7.17−7.38 (m, 7 H), 7.45−7.56 (m, 4 H), 7.75−7.86 (m, 2 H). ^{13}C NMR (75 MHz, THF-d_8): δ 14.35 (q), 24.33 (q, 4 C), 25.05 (q, 4 C), 26.09 (t), 29.97 (d, 4 C), 39.61 (t), 53.05 (t), 124.43 (d, 2 C), 124.78 (d, 4 C), 127.57 (d, 2 C), 128.32 (d, 2 C), 131.04 (d, 2 C), 131.39 (d), 131.76 (s), 136.03 (s), 136.16 (s, 2 C), 146.92 (s, 4 C), 149.93 (s), 154.14 (s), 197.96 (s). HRMS (FAB(+), matrix NPOE): $[C_{40}H_{51}ON_3Au]^+$ calcd 786.3698, found 786.3730. IR (KBr): $\tilde{\nu}$ (cm^{-1}) 3439, 3072, 2962, 2927, 2868, 1633, 1557, 1470, 1460, 1415, 1385, 1364, 1337, 1058, 804, 758, 698, 549, 452, 420.

Synthesis of 4d and 2d. According to GP1, 18.3 mg (85.0 μmol) of *N*-(hept-2-ynyl)benzamide and 51.2 mg (85.0 μmol) of [Au(OH)(IPr)] (**3**) were used. After 1 day, **4d** and **2d** were obtained as a white foam in quantitative yield (**4d**/**2d** = 1/0.12). According to GP2, 32.9 mg (152 μmol) of *N*-(hept-2-ynyl)benzamide was used. After 1 day, **4d** and **2d** were obtained as a white foam in 88% yield (**4d**/**2d** = 0.31/1).

{1,3-Bis[2,6-bis(propan-2-yl)phenyl]-1,3-dihydro-2H-imidazol-2-ylidene}[(1E)-1-(2-phenyl-1,3-oxazol-5(4H)-ylidene)pentyl]gold ***(4d)***. ^{1}H NMR (300 MHz, THF-d_8): δ 0.67 (t, J = 6.9 Hz, 3 H), 0.89−1.14 (m, 4 H), 1.23 (d, J = 6.9 Hz, 12 H), 1.39 (d, J = 6.9 Hz, 12 H), 2.13 (tt, J = 7.3 Hz, J = 2.0 Hz, 2 H), 2.61−2.79 (m, 4 H), 3.84 (t, J = 2.0 Hz, 2 H), 7.16−7.40 (m, 7 H), 7.45−7.57 (m, 4 H), 7.75−7.86 (m, 2 H). ^{13}C NMR (75 MHz, THF-d_8): δ 14.86 (q), 23.47 (t), 24.38 (q, 4 C), 25.01 (q, 4 C), 29.85 (d, 4 C), 34.87 (t), 35.57 (t), 58.96 (t), 124.29 (d, 2 C), 124.76 (d, 4 C), 128.43 (d, 2 C), 128.84 (d, 2 C), 130.75 (s), 131.06 (d, 2 C), 131.20 (d), 136.02 (s), 136.24 (s, 2 C), 147.01 (s, 4 C), 150.52 (s), 163.99 (s), 198.82 (s).

{1,3-Bis[2,6-bis(propan-2-yl)phenyl]-1,3-dihydro-2H-imidazol-2-ylidene}(6-pentyl-2-phenyl-4H-1,3-oxazin-5-yl)gold ***(2d)***. ^{1}H NMR (300 MHz, THF-d_8): δ 0.76 (t, J = 7.3 Hz, 3 H), 0.89−1.14 (m, 4 H), 1.23 (d, J = 6.9 Hz, 12 H), 1.38 (d, J = 6.9 Hz, 12 H), 1.83 (t, J = 7.1 Hz, 2 H), 2.61−2.79 (m, 4 H), 3.67 (s, 2 H), 7.16−7.40 (m, 7 H), 7.45−7.57 (m, 4 H), 7.75−7.86 (m, 2 H). ^{13}C NMR (75 MHz, THF-d_8): δ 14.91 (q), 23.24 (t), 24.33 (q, 4 C), 25.24 (q, 4 C), 29.85 (d, 4 C), 35.40 (t), 37.48 (t), 53.04 (t), 124.44 (d, 2 C), 124.76 (d, 4 C), 127.56 (d, 2 C), 128.32 (d, 2 C), 131.03 (d, 2 C), 131.20 (d), 131.58 (s), 136.02 (s), 136.16 (s, 2 C), 146.90 (s, 4 C), 150.08 (s), 154.12 (s), 197.96 (s). HRMS (FAB(+), matrix NPOE): $[C_{41}H_{53}ON_3Au]^+$ calcd 800.3854, found 800.3872. IR (KBr): $\tilde{\nu}$ (cm^{-1}) 3434, 3421, 2961, 2926, 2869, 1653, 1634, 1471, 1458, 1451, 1414, 1385, 1364, 1337, 1060, 1025, 849, 803, 758, 696.

Synthesis of 4e and 2e. According to GP1, 21.4 mg (85.0 μmol) of 4-bromo-*N*-(but-2-ynyl)benzamide and 51.2 mg (85.0 μmol) of [Au(OH)(IPr)] **3** were used. After 1 day, **4e** and **2e** were obtained as a pale yellow foam in quantitative yield (**4e**/**2e** = 1/0.22). According to GP2, 38.3 mg (152 μmol) of 4-bromo-*N*-(but-2-ynyl)benzamide was used. After 1 day, **4e** and **2e** were obtained as a pale yellow foam in 81% yield (**4e**/**2e** = 0.07/1).

{1,3-Bis[2,6-bis(propan-2-yl)phenyl]-1,3-dihydro-2H-imidazol-2-ylidene}{(1E)-1-[2-(4-bromophenyl)-1,3-oxazol-5(4H)-ylidene]ethyl}gold ***(4e)***. ^{1}H NMR (300 MHz, C_6D_6): δ 0.96 (d, J = 6.9 Hz, 12 H), 1.30 (d, J = 6.9 Hz, 12 H), 2.06 (t, J = 2.5 Hz, 3 H), 2.38 −2.58 (m, 4 H), 4.27 (q, J = 2.5 Hz, 2 H), 6.21 (s, 2 H), 8.87−7.00 (m, 4 H), 7.00−7.09 (m, 2 H), 7.84−7.97 (m, 4 H). ^{13}C NMR (75 MHz, C_6D_6): δ 21.25 (q), 24.03 (q, 4 C), 24.71 (q, 4 C), 29.14 (d, 4 C), 57.64 (t), 122.48 (d, 2 C), 124.41 (d, 4 C), 129.16 (d, 2 C), 130.65 (d, 2 C), 131.04 (d, 2 C), 134.96 (s, 2 C), 136.67 (s), 145.70 (s), 146.01 (s, 4 C), 151.00 (s), 163.40 (s), 169.96 (s), 197.93 (s).

{1,3-Bis[2,6-bis(propan-2-yl)phenyl]-2,3-dihydro-1H-imidazol-2-yl}[2-(4-bromophenyl)-6-methyl-4H-1,3-oxazin-5-yl]gold ***(2e)***. ^{1}H NMR (300 MHz, C_6D_6): δ 0.96 (d, J = 6.9 Hz, 12 H), 1.30 (d, J = 6.9 Hz, 12 H), 2.06 (t, J = 1.5 Hz, 3 H), 2.38−2.58 (m, 4 H), 4.21 (q, J = 1.5 Hz, 2 H), 6.21 (s, 2 H), 8.87−7.00 (m, 4 H), 7.00−7.09 (m, 2 H), 7.84−7.97 (m, 4 H). ^{13}C NMR (75 MHz, C_6D_6): δ 22.10 (q), 23.92 (q, 4 C), 24.66 (q, 4 C), 29.04 (d, 4 C), 52.77 (t), 122.53 (d, 2 C), 124.17 (d, 4 C), 129.14 (d, 2 C), 130.59 (d, 2 C), 131.04 (d, 2 C), 131.91 (s), 132.40 (s), 134.31 (s), 134.93 (s, 2 C), 145.94 (s, 4 C), 146.14 (s), 153.32 (s), 197.96 (s). HRMS (FAB(+), matrix NBA): $[C_{38}H_{46}ON_3{}^{79}BrAu]^+$ calcd 836.2490, found 836.2509. IR (KBr): $\tilde{\nu}$ (cm^{-1}) 2963, 2927, 2868, 2279, 1681, 1592, 1471, 1415, 1385, 1364, 1332, 1285, 1147, 1110, 1092, 1010, 837, 806, 759, 728.

Synthesis of 4f and 2f. According to GP1, 16.3 mg (85.0 μmol) of *N*-(but-2-ynyl)-2,5-dimethylfuran-3-carboxamide and 51.2 mg (85.0 μmol) of [Au(OH)(IPr)] (**3**) were used. After 1 day, **4f** and **2f** were obtained as a pale yellow foam in quantitative yield (**4f**/**2f** = 1/0.14). According to GP2, 19.1 mg (152 μmol) of *N*-(but-2-ynyl)-2,5-dimethylfuran-3-carboxamide was used. After 1 day, **4f** and **2f** were obtained as a pale yellow foam in 76% yield (**4f**/**2f** = 0.17/1).

{1,3-Bis[2,6-bis(propan-2-yl)phenyl]-1,3-dihydro-2H-imidazol-2-ylidene}{(1E)-1-[2-(2,5-dimethylfuran-3-yl)-1,3-oxazol-5(4H)-ylidene]ethyl}gold ***(4f)***. ^{1}H NMR (300 MHz, C_6D_6): δ 1.09 (d, J = 6.9 Hz, 12 H), 1.44 (d, J = 6.9 Hz, 12 H), 1.84 (s, 3 H), 2.16 (t, J = 2.4 Hz, 3 H), 2.47 (s, 3 H), 2.51−2.71 (m, 4 H), 4.36 (q, J = 2.4 Hz, 2 H), 6.37 (s, 2 H), 6.44 (s), 7.08 (d, J = 7.8 Hz, 4 H), 7.27 (t, J = 7.8 Hz, 2 H). ^{13}C NMR (75 MHz, C_6D_6): δ 13.05 (q), 13.65 (q), 21.44 (q), 23.91 (q, 4 C), 24.69 (q, 4 C), 29.04 (d, 4 C), 58.09 (t), 107.01 (d), 112.73 (s), 122.48 (d, 2 C), 124.18 (d, 4 C), 128.15 (s), 130.65 (d, 2 C), 135.02 (s, 2 C), 146.00 (s, 4 C), 149.64 (s), 151.60 (s), 153.17 (s), 160.68 (s), 198.37 (s).

{1,3-Bis[2,6-bis(propan-2-yl)phenyl]-1,3-dihydro-2H-imidazol-2-ylidene}[2-(2,5-dimethylfuran-3-yl)-6-methyl-4H-1,3-oxazin-5-yl]gold ***(2f)***. ^{1}H NMR (300 MHz, C_6D_6): δ 1.08 (d, J = 6.9 Hz, 12 H), 1.41 (d, J = 6.9 Hz, 12 H), 1.80 (t, J = 1.6 Hz, 3 H), 1.89 (s, 3 H), 2.46 (s, 3 H), 2.51−2.71 (m, 4 H), 4.29 (q, J = 1.6 Hz, 2 H), 6.38 (s, 2 H), 6.43 (s), 7.05 (d, 7.8 Hz, 4 H), 7.21 (t, J = 7.8 Hz, 2 H). ^{13}C NMR (75 MHz, C_6D_6): δ 13.13 (q), 13.94 (q), 22.18 (q), 23.94 (q, 4 C), 24.66

(q, 4 C), 29.16 (d, 4 C), 52.40 (t), 107.25 (d), 117.87 (s), 122.55 (d, 2 C), 124.42 (d, 4 C), 130.54 (d, 2 C), 130.90 (s), 134.99 (s, 2 C), 145.96 (s, 4 C), 146.18 (s), 148.48 (s), 151.52 (s), 151.76 (s), 198.26 (s). HRMS (FAB(+), matrix NPOE): $[C_{38}H_{49}O_2N_3Au]^+$ calcd 776.3490, found 776.3436. IR (KBr): $\tilde{\nu}$ (cm^{-1}) 2962, 2925, 2868, 1680, 1585, 1470, 1460, 1415, 1385, 1366, 1349, 1330, 1275, 1226, 1147, 1079, 1042, 1023, 805, 758.

Synthesis of 4g and 2g. According to GP1, 19.7 mg (85.0 μmol) of *N*-(but-2-yn-1-yl)adamantylamide and 51.2 mg (85.0 μmol) of [Au(OH)(IPr)] (**3**) were used. After 1 day, **4g** and **2g** were obtained as a white foam in quantitative yield (**4g**/**2g** = 1/0.15). According to GP2, 35.1 mg (152 μmol) of *N*-(but-2-yn-1-yl)adamantylamide was used. After 1 day, **4g** and **2g** were obtained as a white foam in 58% yield (**4g**/**2g** = 0.50/1).

*{1,3-Bis[2,6-bis(propan-2-yl)phenyl]-1,3-dihydro-2H-imidazol-2-ylidene}{(1E)-1-[2-(tricyclo[3.3.1.1^{3,7}]dec-1-yl)-1,3-oxazol-5(4H)-ylidene]ethyl}gold (**4g**).* ^{1}H NMR (300 MHz, C_6D_6): δ 1.08 (d, *J* = 6.9 Hz, 12 H), 1.41 (d, *J* = 6.9 Hz, 12 H), 1.52−1.58 (m, 6 H), 1.80−1.86 (m, 3 H), 2.05−2.10 (m, 6 H), 2.16 (t, *J* = 2.5 Hz, 3 H), 2.50−2.66 (m, 4 H), 4.24 (q, *J* = 2.5 Hz, 2 H), 6.33 (s, 2 H), 7.05 (d, *J* = 7.5 Hz, 4 H), 7.25 (t, *J* = 7.5 Hz, 2 H). ^{13}C NMR (75 MHz, C_6D_6): δ 21.31 (q), 23.90 (q, 4 C), 24.69 (q, 4 C), 28.53 (d, 3 C), 29.03 (d, 4 C), 36.39 (s), 37.06 (t, 3 C), 39.96 (t, 3 C), 58.10 (t), 122.36 (d, 2 C), 124.15 (d, 4 C), 130.63 (d, 2 C), 173.07 (s), 170.94 (s), 152.30 (s), 145.97 (s, 4 C), 135.00 (s, 2 C), 198.62 (s).

*{1,3-Bis[2,6-bis(propan-2-yl)phenyl]-1,3-dihydro-2H-imidazol-2-ylidene}[6-methyl-2-(tricyclo[3.3.1.1^{3,7}]dec-1-yl)-4H-1,3-oxazin-5-yl]gold (**2g**).* ^{1}H NMR (300 MHz, C_6D_6): δ 1.06 (d, *J* = 6.9 Hz, 12 H), 1.40 (d, *J* = 6.9 Hz, 12 H), 1.52−1.58 (m, 6 H), 1.75−1.81 (m, 3 H), 1.83 (t, *J* = 1.6 Hz, 3 H), 1.98−2.02 (m, 6 H), 2.50−2.66 (m, 4 H), 4.20 (q, *J* = 1.6 Hz, 2 H), 6.33 (s, 2 H), 7.04 (d, *J* = 7.5 Hz, 4 H), 7.16 (t, *J* = 7.5 Hz, 2 H). ^{13}C NMR (75 MHz, C_6D_6): δ 22.18 (q), 24.08 (q, 4 C), 24.67 (q, 4 C), 28.91 (d, 3 C), 29.14 (d, 4 C), 37.45 (t, 3 C), 39.08 (s), 40.64 (t, 3 C), 52.47 (t), 122.44 (d, 2 C), 124.12 (d, 4 C), 130.52 (d, 2 C), 134.97 (s, 2 C), 145.92 (s, 4 C), 146.46 (s), 162.69 (s), 173.06 (s), 198.56 (s). HRMS (FAB(+), matrix NPOE): $[C_{42}H_{57}ON_3Au]^+$ calcd 816.4167, found 816.4158. IR (KBr): $\tilde{\nu}$ (cm^{-1}). 2962, 2905, 2851, 2279, 1689, 1659, 1640, 1455, 1414, 1385, 1365, 1332, 1273, 1144, 1103, 1078, 990, 807, 759.

Synthesis of 4h. According to GP1, 20.0 mg (85.0 μmol) of *N*-(3-phenylprop-2-ynyl)benzamide and 51.2 mg (85.0 μmol) [Au(OH)-(IPr)] (**3**) were used. After 1 day, **4h** was obtained as a pale yellow solid in quantitative yield. According to GP2, 35.8 mg (152 μmol) of *N*-(3-phenylprop-2-ynyl)benzamide was used. After 1 day, **4h** was obtained as a pale yellow solid in 60% yield.

*{1,3-Bis[2,6-bis(propan-2-yl)phenyl]-1,3-dihydro-2H-imidazol-2-ylidene}[(E)-phenyl(2-phenyl-1,3-oxazol-5(4H)-ylidene)methyl]gold (**4h**).* ^{1}H NMR (300 MHz, THF-d_8): δ 1.25 (d, *J* = 6.9 Hz, 12 H), 1.37 (d, *J* = 6.9 Hz, 12 H), 2.64−2.82 (m, 4 H), 4.06 (s, 2 H), 6.71−6.80 (m, 1 H), 6.85−6.94 (m, 2 H), 7.13−7.21 (m, 2 H), 7.29−7.45 (m, 7 H), 7.52−7.62 (m, 4 H), 7.82−7.91 (m, 2 H). ^{13}C NMR (75 MHz, THF-d_8): δ 24.34 (q, 4 C), 24.83 (q, 4 C), 29.79 (d, 4 C), 60.93 (t), 123.56 (d), 124.29 (d, 2 C), 124.78 (d, 4 C), 127.32 (d, 2 C), 128.44 (d, 2 C), 128.92 (d, 2 C), 130.01 (s), 131.04 (d, 2 C), 131.13 (d, 2 C), 131.45 (d), 134.68 (s), 136.13 (s, 2 C), 146.97 (s, 4 C), 147.30 (s), 151.30 (s), 164.20 (s), 196.78 (s). HRMS (FAB(+), matrix NPOE): $[C_{43}H_{49}ON_3Au]^+$ calcd 819.3463, found 819.3451. IR (KBr): ν (cm^{-1}) 3441, 3067, 2962, 2925, 2869, 1745, 1646, 1471, 1415, 1385, 1364, 1332, 1257, 1181, 1061, 1025, 866, 804, 758, 696.

Synthesis of 1,3-Bis[2,6-bis(propan-2-yl)phenyl]-1,3-dihydro-2*H*-imidazol-2-ylidene}[(*E*)-(4-nitrophenyl)(2-phenyl-1,3-oxazol-5(4*H*)-ylidene)methyl]gold (4i). According to GP1, 23.8 mg (85.0 μmol) *N*-(3-(4-nitrophenyl)prop-2-ynyl)benzamide and 51.2 mg (85.0 μmol) [Au(OH)(IPr)] **3** was used. After 1 d, **4i** was obtained as a pale yellow solid in quantitative yield.

^{1}H NMR (300 MHz, THF-d_8): δ 1.26 (d, *J* = 6.9 Hz, 12 H), 1.36 (d, *J* = 6.9 Hz, 12 H), 2.61−2.80 (m, 4 H), 4.07 (s, 2 H), 7.24−7.31 (m, 2 H), 7.32−7.46 (m, 7 H), 7.58−7.68 (m, 4 H), 7.77−7.83 (m, 2 H), 7.84−7.91 (m, 2 H). ^{13}C NMR (75 MHz, THF-d_8): δ 24.29 (q, 4 C), 24.86 (q, 4 C), 29.82 (d, 4 C), 61.46 (t), 122.92 (d, 2 C), 124.50 (d, 2 C), 124.90 (d, 4 C), 128.48 (d, 2 C), 129.14 (d, 2 C), 129.28 (s), 131.10 (d, 2 C), 131.21 (d, 2 C), 131.90 (d), 133.24 (s), 135.99 (s, 2 C), 144.51 (s), 147.05 (s, 4 C), 155.41 (s), 155.45 (s), 164.01 (s), 195.35 (s). HRMS (FAB(+), matrix NPOE): $[C_{43}H_{48}O_3N_4Au]^+$ calcd 865.3392, found 865.3392. IR (KBr): $\tilde{\nu}$ (cm^{-1}) 3426, 2962, 2926, 2869, 1652, 1582, 1499, 1471, 1417, 1385, 1325, 1107, 1075, 1059, 1025, 850, 804, 758, 696.

Synthesis of 7i and 4i. According to GP1, 14.5 mg (52.0 μmol) of *N*-(3-(4-nitrophenyl)prop-2-ynyl)benzamide and 31.3 mg (52.0 μmol) of [Au(OH)(IPr)] (**3**) were used. After 30 min at room temperature, the mixture was measured in NMR at −80 °C. After the intermediate amide complex **7i** was characterized, the solution was measured for 16 h with continuous ^{1}H NMR to investigate the conversion of the amide complex **7i** to vinylgold intermediate **4i**.

*{1,3-Bis[2,6-bis(propan-2-yl)phenyl]-1,3-dihydro-2H-imidazol-2-ylidene}{N-[3-(4-nitrophenyl)prop-2-yn-1-yl]benzamidato-κN}gold (**7i**).* ^{1}H NMR (300 MHz, THF-d_8): δ 0.88−1.44 (m, 24 H), 2.33−2.63 (m, 4 H), 1.12 (s, 2 H), 6.79 (t, *J* = 7.4 Hz, 2 H), 7.09 (t, *J* = 6.91 Hz, 1 H), 7.29−7.50 (m, 6 H), 7.53−7.71 (m, 4 H), 7.88 (s, 2 H), 8.32 (d, *J* = 8.5, 2 H). ^{13}C NMR (75 MHz, THF-d_8): δ 23.99 (q, 4 C), 24.95 (q, 4 C), 29.67 (d, 4 C), 38.51 (t), 79.05 (s), 97.60 (s), 124.42 (d, 2 C), 125.10 (d, 4 C), 125.21 (d, 2 C), 128.05 (d, 2 C), 128.19 (d, 2 C), 128.90 (d), 131.43 (d, 2 C), 132.32 (s), 133.63 (d, 2 C), 135.36 (s, 2 C), 142.67 (s), 146.27 (s, 4 C), 147.22 (s), 174.56 (s), 174.96 (s).

Synthesis of 7k and 4k. According to GP1, 21.5 mg (85.0 μmol) of *N*-(3-(5-formylfuran-2-yl)prop-2-ynyl)benzamide and 51.2 mg (12.3 μmol) of [Au(OH)(IPr)] (**3**) were used. After 1 day, the conversion of the amide complex was not complete, and so both amide complex **7k** and vinylgold intermediate **4k** were analyzed by NMR. After an additional 2 days the conversion to vinylgold intermediate **4k** was complete and the product was obtained as a pale yellow solid in quantitative yield.

*{1,3-bis[2,6-bis(propan-2-yl)phenyl]-1,3-dihydro-2H-imidazol-2-ylidene}{N-[3-(5-formylfuran-2-yl)prop-2-yn-1-yl]benzamidato-κN} gold (**7k**).* ^{1}H NMR (300 MHz, THF-d_8): δ 1.17 (d, *J* = 6.9 Hz, 12 H), 1.21 (d, *J* = 6.9 Hz, 12 H), 2.50−2.66 (m, 4 H), 4.14 (s, 2 H), 6.61 (d, *J* = 3.6 Hz, 1 H), 6.75 (t, *J* = 7.6 Hz, 2 H), 7.01 (t, *J* = 7.6 Hz, 1 H), 7.56 (s, 2 H), 7.26−7.60 (m, 9 H), 9.57 (s, 1 H). ^{13}C NMR (75 MHz, THF-d_8): δ 24.23 (q, 4 C), 24.65 (q, 4 C), 29.70 (d, 4 C), 38.55 (t), 70.24 (s), 100.05 (s), 116.79 (d), 124.89 (d, 2 C), 125.05 (d, 4 C), 126.43 (d), 127.85 (d, 2 C), 128.16 (d, 2 C), 128.46 (d), 131.39 (d, 2 C), 135.63 (s, 2 C), 143.36 (s), 143.80 (s), 146.49 (s, 4 C), 153.21 (s), 175.39 (s), 176.59 (s), 177.19 (d).

*{1,3-Bis[2,6-bis(propan-2-yl)phenyl]-1,3-dihydro-2H-imidazol-2-ylidene}[(E)-(5-formylfuran-2-yl)(2-phenyl-1,3-oxazol-5(4H)-ylidene)methyl]gold (**4k**).* ^{1}H NMR (300 MHz, THF-d_8): δ 1.26 (d, *J* = 6.9 Hz, 12 H), 1.41 (d, *J* = 6.9 Hz, 12 H), 2.65−2.82 (m, 4 H), 4.06 (s, 2 H), 6.26 (d, *J* = 3.6 Hz, 1 H), 7.03 (d, *J* = 3.6 Hz, 1 H), 7.36−7.48 (m, 7 H), 7.56 (t, *J* = 8.0 Hz, 2 H), 7.62 (s, 2 H), 7.92−8.02 (m, 2 H), 9.30 (s, 1 H). ^{13}C NMR (75 MHz, THF-d_8): δ 24.26 (q, 4 C), 25.01 (q, 4 C), 29.83 (d, 4 C), 61.80 (t), 110.91 (d), 120.74 (s), 124.55 (d), 124.84 (d, 4 C), 128.62 (d, 2 C), 129.15 (d), 129.18 (d, 2 C), 131.13 (d, 2 C), 131.97 (d, 2 C), 135.98 (s, 2 C), 146.98 (s, 4 C), 150.94 (s), 157.47 (s), 164.16 (s), 166.94 (s), 176.58 (s), 176.64 (d), 194.65 (s). HRMS (FAB(+), matrix NPOE): $[C_{42}H_{47}O_3N_3Au]^+$ calcd 838.3283, found 838.3292. IR (KBr): $\tilde{\nu}$ (cm^{-1}) 3434, 2962, 2926, 2869, 1653, 1616, 1553, 1471, 1417, 1386, 1364, 1328, 1214, 1076, 1059, 1025, 917, 803, 757, 696.

Synthesis of *p*-Bis{1,3-bis[2,6-bis(propan-2-yl)phenyl]-1,3-dihydro-2*H*-imidazol-2-ylidene}[(*E*)-phenyl(1,3-oxazol-5(4*H*)-ylidene)methyl]gold}benzene (6). According to GP1, 10.2 mg (52.0 μmol) of *N*1,*N*4-bis(3-phenylprop-2-ynyl)terephthalamide and 62.6 mg (104 μmol) of [Au(OH)(IPr)] (**3**) was used. After 1 day, **6** was obtained as a pale yellow solid in quantitative yield.

^{1}H NMR (300 MHz, THF-d_8): δ 1.23 (d, *J* = 6.9 Hz, 24 H), 1.35 (d, *J* = 6.9 Hz, 24 H), 2.62−2.80 (m, 8 H), 4.04 (s, 4 H), 6.70−6.79 (m, 2 H), 6.83−6.92 (m, 4 H), 7.09−7.17 (m, 4 H), 7.35−7.43 (m, 8 H), 7.52−7.61 (m, 8 H), 7.84 (s, 4 H). ^{13}C NMR (75 MHz, THF-d_8): δ 24.45 (q, 8 C), 24.93 (q, 8 C), 29.91 (d, 8 C), 61.09 (t, 2 C), 123.73 (d, 2 C), 124.42 (d, 4 C), 124.90 (d, 8 C), 127.46 (d, 4 C), 128.34 (d, 4 C), 131.16 (d, 4 C), 131.21 (d, 4 C), 132.03 (s, 2 C), 135.05 (s, 2 C), 136.23 (s, 4 C), 147.08 (s, 8 C), 147.27 (s, 2 C), 151.14 (s, 2 C),

dx.doi.org/10.1021/om2009556|*Organometallics* 2011, 30, 6328−6337

163.99 (s, 2 C), 196.81 (s, 2 C). HRMS (FAB(+), matrix NPOE): $[C_{80}H_{91}O_2N_6Au_2]^+$ calcd 1561.6535, found 1561.6538. IR (KBr): $\tilde{\nu}$ (cm^{-1}) 2962, 2926, 2868, 1648, 1622, 1592, 1486, 1470, 1414, 1385, 1364, 1327, 1254, 1214, 1062, 1019, 864, 803, 758, 694.

Synthesis of {1,3-Bis[2,6-bis(propan-2-yl)phenyl]-imidazolidin-2-ylidene}(4-methylphenolato)gold ([Au(O-*p*-Tol)(IPr)]). [Au(OH)(IPr)] (**3**; 50 mg, 0.083 mmol) and *p*-cresol (9.0 mg, 0.083 mmol) were introduced into a vial containing toluene (0.8 mL). The reaction mixture was stirred at 60 °C for 14 h. The reaction mixture was cooled to room temperature, and the solvent volume was reduced by half, under vacuum. Pentane (6 mL) was added, and the resulting precipitate was collected on a frit and washed with pentane (3 × 3 mL). The solid was dried under vacuum to afford [Au(O-*p*-Tol)(IPr)] as a white microcrystalline solid (51.1 mg, 89%).

^{1}H NMR (300 MHz, CD_2Cl_2): δ 7.58 (t, J = 7.8 Hz, 2H, C*H* aromatic), 7.36 (d, J = 7.8 Hz, 4H, C*H* aromatic), 7.26 (s, 2H, C*H* imidazole), 6.59 (br d, J = 8.2 Hz, 2H, C*H* *p*-cresol), 6.10 (*br* d, J = 8.2 Hz, 2H, C*H* *p*-cresol), 2.60 (sept, J = 6.9 Hz, 4H, C*H*(CH_3)$_2$), 2.07 (s, 3H, CH_3 *p*-cresol), 1.34 (d, J = 6.9 Hz, 12H, CH(CH_3)$_2$), 1.23 (d, J = 6.9 Hz, 12H, CH(CH_3)$_2$). ^{13}C NMR (75 MHz, CD_2Cl_2): δ 169.8 (s, *C* carbene), 166.0 (s, *C* aromatic *p*-cresol), 146.3 (s, *C* aromatic NHC), 134.7 (s, *C* aromatic), 131.0 (s, *C*H imidazole), 129.2 (s, *C*H aromatic *p*-cresol), 124.6 (s, *C*H aromatic), 123.7 (s, *C*H aromatic), 123.4 (s, *C* aromatic *p*-cresol), 118.1 (s, *C*H aromatic *p*-cresol), 29.2 (s, *C*H(CH_3)$_2$), 24.5 (s, CH(*C*H_3)$_2$), 24.3 (s, CH(*C*H_3)$_2$), 20.3 (s, *C*H_3 *p*-cresol) ppm. Anal. Calcd for $C_{34}H_{43}AuN_2O$: C, 58.95; H, 6.26; N, 4.04. Found: C, 59.21; H, 6.58; N, 3.91.

Synthesis of {1,3-Bis[2,6-bis(propan-2-yl)phenyl]-imidazolidin-2-ylidene}(4-methylanilinato)gold ([Au(NH-*p*-Tol)(IPr)]). [Au(OH)(IPr)] (**3**; 50 mg, 0.083 mmol) and *p*-toluidine (8.9 mg, 0.083 mmol) were introduced into a vial containing toluene (0.8 mL). The reaction mixture was stirred at 100 °C for 24 h. The reaction mixture was cooled to room temperature, at which point the solvent volume was reduced by half, under vacuum. Pentane (6 mL) was added, and the resulting precipitate was collected on a frit and washed with pentane (3 × 3 mL). The solid was dried under vacuum to afford [Au(NH-*p*-Tol)(IPr)] as a brown microcrystalline solid (49 mg, 85%).

^{1}H NMR (400 MHz, C_6D_6): δ 7.29 (t, J = 7.8 Hz, 2H, C*H* aromatic), 7.11 (d, J = 7.8 Hz, 4H, C*H* aromatic), 6.85 (br d, J = 8.1 Hz, 2H, C*H* *p*-toluidine), 6.30 (s, 2H, C*H* imidazole), 6.22 (br d, J = 7.9 Hz, 2H, C*H* *p*-toluidine), 3.49 (br s, 1H, N*H* *p*-toluidine), 2.62 (sept, J = 6.9 Hz, 4H, C*H*(CH_3)$_2$), 2.31 (s, 3H, CH_3 *p*-toluidine), 1.41 (d, J = 6.9 Hz, 12H, CH(CH_3)$_2$), 1.07 (d, J = 6.9 Hz, 12H, CH(CH_3)$_2$) ppm. ^{13}C NMR (100 MHz, C_6D_6): δ 182.4 (s, *C* carbene), 157.5 (s, *C* *p*-toluidine), 146.2 (s, *C* aromatic NHC), 135.0 (s, *C*H aromatic NHC), 130.6 (s, *C*H imidazole), 129.3 (s, *C*H *p*-toluidine), 124.4 (s, *C*H aromatic NHC), 122.2 (s, *C*H aromatic NHC), 119.3 (s, *C* *p*-toluidine), 115.2 (s, *C*H *p*-toluidine), 29.1 (s, *C*H(CH_3)$_2$), 24.6 (s, CH(*C*H_3)$_2$), 24.0 (s, CH(*C*H_3)$_2$), 20.9 (s, *C*H_3 *p*-toluidine) ppm. Anal. Calcd for $C_{34}H_{44}AuN_3$: C, 59.04; H, 6.41; N, 6.07. Found: C, 58.70; H, 6.31; N, 6.14.

■ ASSOCIATED CONTENT

Ⓢ Supporting Information

Text, tables, and figures giving an Arrhenius plot for the formation of vinylgold(I) complex **4i**, a detailed procedure for the synthesis of IPrAuOH (**3**) on a large scale, calculations for a mechanism involving **3** and cationic gold(I) species, and ^{1}H and ^{13}C NMR spectra of complexes **2**–**4**, **6**, **7**, [Au(O-*p*-Tol)(IPr)], and [Au(O-*p*-Tol)(IPr)]. This material is available free of charge via the Internet at http://pubs.acs.org.

■ AUTHOR INFORMATION

Corresponding Author

*E-mail: snolan@st-andrews.ac.uk (S.P.N.); hashmi@hashmi.de (A.S.K.H.).

■ ACKNOWLEDGMENTS

The ERC (FUNCAT to SPN) and the EPSRC are gratefully acknowledged for support of this work. A.P. thanks the Spanish MICINN for a Ramón y Cajal contract (RYC-2009-04170). Umicore AG and Chemetall AG are thanked for their generous gifts of materials. S.P.N. is a Royal Society Wolfson Research Merit Award holder. We thank Dr. Pierrick Nun for valuable discussions.

■ REFERENCES

(1) (a) Nolan, S. P. *Acc. Chem. Res.* **2011**, *44*, 91–100. (b) López, F.; Mascareñas, J. L. *2011 Beilstein J. Org. Chem.* **2011**, *7*, 1075–1094. (c) Rudolph, M.; Hashmi, A. S. K. *Chem. Commun.* **2011**, *47*, 6536–6544. (d) Sengupta, S.; Shi, X. *ChemCatChem* **2010**, *2*, 609–619. (e) Fürstner, A. *Chem. Soc. Rev.* **2009**, *38*, 3208–3221. (f) Garcia, P.; Malacria, M.; Aubert, C.; Gandon, V.; Fensterbank, L. *ChemCatChem* **2010**, *2*, 493–497. (g) Hashmi, A. S. K. *Chem. Rev.* **2007**, *107*, 3180–3211. (h) Gorin, D. J.; Sherry, B. D.; Toste, F. D. *Chem. Rev.* **2008**, *108*, 3351–3378. (i) Li, Z.; Brouwer, C.; He, C. *Chem. Rev.* **2008**, *108*, 3239–3265. (j) Arcadi, A. *Chem. Rev.* **2008**, *108*, 3266–3325. (k) Jiménez-Núñez, E.; Echavarren, A. M. *Chem. Rev.* **2008**, *108*, 3326–3350. (l) Muzart, J. *Tetrahedron* **2008**, *64*, 5815–5849. (m) Patil, N. T.; Yamamoto, Y. *Chem. Rev.* **2008**, *108*, 3395–3442. (n) Skouta, R.; Li, C.-J. *Tetrahedron* **2008**, *64*, 4917–4918. (o) Shen, H. C. *Tetrahedron* **2008**, *64*, 3885–3903. (p) Hashmi, A. S. K.; Rudolph, M. *Chem. Soc. Rev.* **2008**, *37*, 1766–1775. (q) Fürstner, A.; Davies, P. W. *Angew. Chem., Int. Ed.* **2007**, 3410–3449. (r) Jiménez-Núñez, E.; Echavarren, A. M. *Chem. Commun.* **2007**, 333–346. (s) Hashmi, A. S. K.; Hutchings, G. J. *Angew. Chem., Int. Ed.* **2006**, *45*, 7896–7936. (t) Zhang, L.; Sun, J.; Kozmin, S. A. *Adv. Synth. Catal.* **2006**, *248*, 2271–2296. (u) Malacria, M.; Goddard, J.-P.; Fensterbank, L. In *Comprehensive Organometallic Chemistry*, 3rd ed.; Crabtree, R.; Mingos, M., Eds.; Elsevier: Amsterdam, 2006; Vol. *10*, Chapter 10.07, p 299. (v) Widenhoefer, R. A.; Han, X. *Eur. J. Org. Chem.* **2006**, 4555–4563.

(2) For cationic gold(I) complexes coordinated to alkynes, see: (a) Hooper, T. N.; Green, M.; Russel, C. A. *Chem. Commun.* **2010**, *46*, 2313–2315. (b) Flügge, S.; Anoop, A.; Goddard, R.; Thiel, W.; Fürstner, A. *Chem. Eur. J.* **2009**, *15*, 8558–8565. (c) Lavallo, V.; Frey, G. D.; Donnadieu, B.; Soleilhavoup, M.; Bertrand, G. *Angew. Chem., Int. Ed.* **2008**, *47*, 5224–5228. For cationic gold(I) complexes coordinated to alkenes, see: (d) Brown, T. J.; Dickene, M. G.; Widenhoefer, R. A. *J. Am. Chem. Soc.* **2009**, *131*, 6350–6351. (e) Brown, T. J.; Dickene, M. G.; Widenhoefer, R. A. *Chem. Commun.* **2009**, 6451–6453. (f) Hooper, T. N.; Green, M.; McGrady, J. E.; Patel, J. R.; Russel, C. A. *Chem. Commun.* **2009**, 3877–3879. (g) de Frémont, P.; Marion, N.; Nolan, S. P. *J. Organomet. Chem.* **2009**, *694*, 551–560. For cationic gold(I) complexes coordinated to allenes, see: (h) Brown, T. J.; Sugie, A.; Dickene, M. G.; Widenhoefer, R. A. *Organometallics* **2010**, *29*, 4207–4209. For cationic gold complexes coordinated to arenes, see: (i) Herreo-Gómez, E.; Nieto-Oberhuber, C.; López, S.; Benet-Buchholz, J.; Echavarren, A. M. *Angew. Chem., Int. Ed.* **2006**, *45*, 5455–5459.

(3) For a review and discussion on recent isolated intermediates involved in gold homogeneous catalysis, see: (a) Hashmi, A. S. K. *Angew. Chem., Int. Ed.* **2010**, *49*, 5232–5241. For a more recent example, see: (b) Melchionna, M.; Nieger, M.; Helaja, J. *Chem. Eur. J.* **2010**, *16*, 8262–8267.

(4) (a) Weyrauch, J. P.; Hashmi, A. S. K.; Schuster, A.; Hengst, T.; Schetter, S.; Littmann, A.; Rudolph, M.; Hamzic, M.; Visus, J.; Rominger, F.; Frey, W.; Bats, J. W. *Chem. Eur. J.* **2010**, *16*, 956–963. (b) Hashmi, A. S. K.; Rudolph, M.; Schymura, S.; Visus, J.; Frey, W. *Eur. J. Org. Chem.* **2006**, 4905–4909. (c) Hashmi, A. S. K.; Weyrauch, J. P.; Frey, W.; Bats, J. W. *Org. Lett.* **2004**, *6*, 4391–4394. For other studies on gold-catalyzed oxazole synthesis from propargyl carboxamide, see: (d) Milton, M. D.; Inada, Y.; Nishibayashi, Y.; Uemura, S. *Chem. Commun.* **2004**, 2712–2713.

(5) (a) Hashmi, A. S. K.; Ramamurthi, T. D.; Rominger, F. *Adv. Synth. Catal.* **2010**, *352*, 971−975. (b) Hashmi, A. S. K.; Ramamurthi, T. D.; Rominger, F. *J. Organomet. Chem.* **2009**, *694*, 592−597. (c) Hashmi, A. S. K. *Gold Bull.* **2009**, *42*, 275−279. (d) Hashmi, A. S. K.; Schuster, A. M.; Rominger, F. *Angew. Chem., Int. Ed.* **2009**, *48*, 8247−8249. For previously reported vinylgold(I) complexes, see: (e) Weber, D.; Tarselli, M. A.; Gagné, M. R. *Angew. Chem., Int. Ed.* **2009**, *48*, 5733−5736. (f) Liu, L.-P.; Xu, B.; Mashuta, M. S.; Hammond, G. B. *J. Am. Chem. Soc.* **2008**, *130*, 17642−17643. (g) Mohr, F.; Falvello, L. R.; Laguna, M. *Eur. J. Inorg. Chem.* **2006**, 833−838.

(6) Gaillard, S.; Slawin, A.M. Z.; Nolan, S. P. *Chem. Commun.* **2010**, *46*, 2742−2744.

(7) (a) Ramón, R. S.; Gaillard, S.; Poater, A.; Cavallo, L.; Slawin, A. M. Z.; Nolan, S. P. *Chem. Eur. J.* **2011**, *17*, 1238−1246. (b) Gaillard, S.; Nun, P.; Slawin, A. M. Z.; Nolan, S. P. *Organometallics* **2010**, *29*, 5402−5408. (c) Ramón, R. S.; Gaillard, S.; Slawin, A. M. Z.; Porta, A.; D'Alfonso, A.; Zanoni, G.; Nolan, S. P. *Organometallics* **2010**, *29*, 3665−3668. (d) Fortman, G. C.; Poater, A.; Levell, J. W.; Gaillard, S.; Slawin, A. M. Z.; Samuel, I. D. W.; Cavallo, L.; Nolan, S. P. *Dalton Trans.* **2010**, *39*, 10382−10390.

(8) For organic transformations catalyzed by [Au(NHC)(OH)]-acid activation, see: (a) Merlini, V.; Gaillard, S.; Porta, A.; Zanoni, G.; Vidari, G.; Nolan, S. P. *Tetrahedron Lett.* **2011**, *52*, 1124−1127. (b) Nun, P.; Gaillard, S.; Poater, A.; Cavallo, L.; Nolan, S. P. *Org. Biomol. Chem.* **2011**, *9*, 101−104. (c) Nun, P.; Ramón, R. S.; Gaillard, S.; Nolan, S. P. *J. Organomet. Chem.* **2011**, *696*, 7−11. (d) Nun, P.; Gaillard, S.; Slawin, A. M. Z.; Nolan, S. P. *Chem. Commun.* **2010**, *46*, 9113−9115. (e) Gaillard, S.; Bosson, J.; Ramón, R. S.; Nun, P.; Slawin, A. M. Z.; Nolan, S. P. *Chem. Eur. J.* **2010**, *16*, 13729−13740. For an interesting [Au(IPr)(OH)]-catalyzed organic transformation, see: (f) Boogaerts, I. I.; Nolan, S. P. *J. Am. Chem. Soc.* **2010**, *132*, 8858−8859.

(9) (a) Hashmi, A. S. K.; Frost, T. M.; Bats, J. W. *Org. Lett.* **2001**, *3*, 3769−3771. (b) Hashmi, A. S. K.; Enns, E.; Frost, T. M.; Schäfer, S.; Schuster, A.; Frey, W.; Rominger, F. *Synthesis* **2008**, 2707−2718. (c) Zhang, Y.; Xin, Z.-J.; Xue, J.-J.; Li, Y. *Chin. J. Chem.* **2008**, *26*, 1461−1464.

(10) *p*-cresol and *p*-toluidine in the presence of complex **3** were deprotonated to afford the *O*-[Au(IPr)] and the *N*-[Au(IPr)] complexes in 89% and 85% isolated yields, respectively.

(11) The DFT optimizations were performed with the BP86 GGA functional using the SDD ECP on Au and the SVP basis set on all main-group atoms. The reported energies have been optimized via single-point calculations on the BP86 geometries using the M06 functional. Solvent effects (THF) were introduced with the PCM approach.